Prediction of the Oral Absorption of Low-Permeability Drugs Using Small Intestine-Like 2/4/A1 Cell Monolayers

Staffan Tavelin,[1,3] Jan Taipalensuu,[1] Lauri Söderberg,[1] Rick Morrison,[2] Saeho Chong,[2] and Per Artursson[1,3,4]

Received October 30, 2002; accepted December 6, 2002

Purpose. To characterize the paracellular route of 2/4/A1 monolayers and to compare the permeabilities of incompletely absorbed oral drugs in 2/4/A1 with those in Caco-2 monolayers.

Methods. The cells were cultivated on permeable supports. The 2/4/A1 expression of genes associated with tight junctions was compared with that in the small intestine using RT-PCR. The aqueous pore radii were determined using paracellular marker molecules. The permeabilities of a series of incompletely absorbed drugs (defined as having a fraction absorbed 0 to 80%) after oral administration to humans were studied.

Results. Occludin and claudin 1 and 3 were expressed in 2/4/A1. The pore radius of 2/4/A1 was 9.0 ± 0.2 Å, which is similar to that in the human small intestine, although the pore radius was smaller (3.7 ± 0.1 Å) in Caco-2. The relationship between permeability and fraction absorbed of 13 drugs was stronger in 2/4/A1 than in Caco-2. The relationships were used to predict the intestinal absorption of another seven drugs. The prediction was more accurate in 2/4/A1 (RMSE = 15.6%) than in Caco-2 (RMSE = 21.1%). Further, Spearman's rank coefficient between FA and permeability was higher in 2/4/A1.

Conclusion. The improved 2/4/A1 cell culture model has a more *in vivo*-like permeability and predicted the oral absorption of incompletely absorbed drugs better than Caco-2 cells.

KEY WORDS: prediction; drug absorption; Caco-2; paracellular; intestinal epithelia.

INTRODUCTION

The Caco-2 model is used for qualitative and sometimes also quantitative prediction of passive human intestinal permeability to drug-like molecules in drug discovery and development (1–4). However, the quality of the results varies with the compounds studied. Good quantitative to semiquantitative results are obtained when analogous series of drugs that are relatively well absorbed are studied. Such drugs are transported mainly via the transcellular route. However, when incompletely absorbed drugs that have low permeability coefficients (e.g., drugs that are at least partly transported via the paracellular route) are investigated, the results become more scattered and qualitative rather than quantitative.

This is at least partly explained by the fact that Caco-2 cells form less permeable tight junctions than those found in the human small intestinal epithelium, and this results in very low paracellular permeability for the Caco-2 cell monolayers. One difference between the tight junctions in Caco-2 cell monolayers and those in the human small intestine, for example, is a difference in average pore radius (5). Thus, the paracellular permeability of Caco-2 cell monolayers more closely resembles that of the human colon than that of the human small intestine (5,6). In fact, the permeability coefficients of low-permeability drugs and markers can be up to 100 times lower in Caco-2 monolayers than they are in the small intestine *in vivo* (6). It is clear that Caco-2 cells may not be quantitatively predictive of the intestinal absorption for drugs that are absorbed via the paracellular route *in vivo*, especially because orally administered drugs are absorbed predominantly from the small intestine. In addition, the low paracellular permeability of Caco-2 cells causes technical and analytic problems that contribute to the scattered results obtained for this group of compounds. A third, less general explanation is transport of poorly permeable compounds by an active transport mechanism that is more abundantly expressed in the intestinal epithelium than in Caco-2 cells (7).

Qualitative results (e.g., classification of compounds into high- and low-permeability drugs) may be sufficient in early screening of libraries of drug-like compounds. However, more quantitative results would be advantageous because such results would result in a better ranking of the individual compounds. Research on cell culture models that better reflect both the transcellular and the paracellular permeability of the human small intestine is therefore of interest. Furthermore, research using cell culture models that more closely resemble the human small intestine will provide both fundamental and applied mechanistic information concerning the role of the paracellular route in drug absorption.

A particularly interesting cell line in this regard is 2/4/A1, a rat intestinal epithelial cell line, which forms polarized monolayers 4–6 days after seeding onto permeable supports (8,9). Initial results showed that the permeability of 2/4/A1 monolayers is comparable to that of the human small intestine (9). This led us to pose the hypothesis that 2/4/A1 cell monolayers are a suitable cell model for studies of slowly and incompletely absorbed drugs that are significantly transported via the paracellular route. Drugs transported via this mechanism include drugs such as atenolol (10,11), H_2 antagonists (12,13), furosemide (14,15), and hydrophilic peptides (5,16,17).

We have determined the levels of mRNA that code for various proteins associated with tight junctions in 2/4/A1 cell monolayers in order to characterize the paracellular route in these cells. The 2/4/A1 cell monolayers were cultivated using a new optimized cell culture procedure that enabled us to grow the cells at 39°C, where the cells are in their most differentiated state. The optimized procedure is presented in detail in an accompanying paper (8). We have subsequently determined the average aqueous pore radii of the tight junctions in 2/4/A1 and Caco-2 cell monolayers and compared them. Furthermore, we have established relationships between the absorbed fractions of a set of incompletely absorbed drugs after oral administration to humans (FA) and monolayer permeabilities in 2/4/A1 and Caco-2 cell monolayers. Finally, we have used these relationships to predict the human intestinal absorption of a second set of incompletely

[1] Department of Pharmacy, Uppsala University, SE-751 23 Uppsala, Sweden.

[2] Bristol-Myers Squibb Co., Pharmaceutical Research Institute, Department of Metabolism & Pharmacokinetics, Princeton, New Jersey 08543.

[3] Center of Pharmaceutical Informatics.

[4] To whom correspondence should be addressed. (e-mail: per.artursson@farmaci.uu.se)

ABBREVIATION: Å, Angstrom (1×10^{-10} m)

0724-8741/03/0300-0397/0 © 2003 Plenum Publishing Corporation

absorbed drugs. In summary, 2/4/A1 cell monolayers have a paracellular permeability that better reflects the human situation than that of Caco-2 cell monolayers. This *in vivo*-like paracellular permeability makes 2/4/A1 cell monolayers an interesting alternative to Caco-2 cells and artificial membranes for the prediction of human intestinal passive permeability, especially to incompletely absorbed drugs.

MATERIALS AND METHODS

Cell Culture

Culture media and supplements were purchased from Gibco BRL Life Technologies AB (Täby, Sweden) unless otherwise stated. 2/4/A1 cells [which originate from fetal rat intestine and are conditionally immortalized with a pZipSVtsa58 plasmid containing a temperature-sensitive mutant of the SV40 large T antigen (18)] were expanded as described in the accompanying paper (8). The medium was changed every second day, and the cells were passaged at 80% confluence, approximately every fourth day.

For functional studies, 2/4/A1 cells were seeded at 100,000 cells/cm^2. The cells were grown in RPMI 1640 supplemented with 6% fetal calf serum (FCS), growth factors, penicillin (100 U/ml), and streptomycin 100 (μg/ml) on Transwell polycarbonate filters (0.45-μm pore size, 12 mm in diameter; Costar, Cambridge, MA) coated with EHS extracellular matrix (Promega Corporation, Madison, WI). Cells were used between passage number 23 and 43.

Caco-2 cells were cultivated as described previously (19,20). The 2/4/A1 and Caco-2 cultures were tested negative for *Mycoplasma* contamination every second month throughout this study.

RT-PCR of Transcripts Coding for Tight Junction Proteins

For the characterization of transcripts coding for tight junction proteins, approximately 7×10^6 filter-grown 2/4/A1 cells were harvested using ice-cold phosphate-buffered saline solution and a cell scraper. Cells were kept on ice during the scraping procedure and subsequently recovered by centrifugation. 2/4/A1 cells and the rat ileal tissue (positive control) were homogenized using a Heidolph DIAX 900 tissue homogenizer equipped with a 6G tool (Heidolph Instruments, Cinnaminson, NJ). RNA was extracted and checked for absence of contaminating genomic DNA, as previously described (21). Also, PCR primer design (Table I) and reaction conditions were as previously described by Taipalensuu *et al.* (21), except that no additional 5′ sequence was added to the PCR primers, and all PCR cycles were conducted at an annealing temperature of 56°C. Samples were analyzed after 25, 29, 33, and 37 PCR cycles.

Selection of Drugs

Drugs that are reported in the literature to be predominantly absorbed by passive diffusion from the human intestine were identified as described previously (22). Briefly, drugs whose bioavailability is limited by solubility and presystemic metabolism were excluded unless these could be accounted for. In particular, drugs that have a fraction absorbed (FA) of less than or equal to 80% were included in this study. This cutoff value constitutes the border between high- and low-permeability drugs according to Winiwarter *et al.* (23). However, in order to study the performance of 2/4/A1 monolayers over the entire absorption range, seven drugs with FA 80–100% were also considered initially. In total, 20 drugs were investigated in this part of the study. Eight of these drugs were categorized as sparingly absorbed (FA = 0–20%), five drugs were categorized as intermediately absorbed (FA = 20–80%), and seven drugs were categorized as completely absorbed (FA = 80–100%) across the human intestine.

The sparingly and intermediately absorbed drugs (13 drugs; FA = 0–80%) were subsequently extracted from the data set and used as a training set in order to establish a relationship between permeability and FA. These drugs are listed in Table II. A second set of seven drugs (FA = 0 to 80%) (Table III) was finally selected as an *ad hoc* test set in order to validate the 2/4/A1 and Caco-2 cell monolayers. The *ad hoc* test set was chosen on the basis of observed poor performance of Caco-2 in predicting the *in vivo* permeability or FA for these drugs (Saeho Chong, unpublished results).

The molecular diversity of the data sets was analyzed by principal component analysis (PCA) in SIMCA-P 8.0 using default settings (24). This analysis was performed using the calculated descriptors molecular weight, total surface area and volume (descriptors of molecular size), ClogP, $NPSA_{saturated}$, $NPSA_{unsaturated}$, and NPSA (descriptors of hydrophobicity), and PSA and fraction PSA (descriptors of hydrophilicity) for the 13 drugs in the training set and five of the seven drugs in the *ad hoc* test set.

Drugs

[^{14}C]Acyclovir, [^{14}C]ganciclovir, [^{14}C]PEG (MW 4000), and [^{14}C]phosphonoformic acid were purchased from Moravec Biochemicals (Brea, CA). Acyclovir, atenolol, lactulose, metolazone, phosphonoformic acid, and sulpiride were obtained from Sigma (St. Louis, MO). [^{14}C]Clodronate and unlabeled clodronate (Leiras Co., Turku, Finland) were gifts from Dr. J. Mönkkönen (University of Kuopio, Finland). [^{14}C]Mannitol, [^{3}H]raffinose, and [^{3}H]vasopressin were obtained from New England Nuclear (Boston, MA). [^{3}H]Lactulose was obtained from American Radiolabeled Chemicals Inc. (St. Louis, MO). BMS 189664, BMS 187745, didanosine,

Table I. Gene-Specific PCR Primers

Gene	Forward primer	Reverse primer	Expected fragment length
Occludin	5′-AATGGCATACTCCTCCAACG	5′-AGTCATCCACGGACAAGGTC	125
Claudin 1	5′-TTAGTGGCCACAGCATGGTA	5′-GAAGGTGTTGGCTTGGGATA	215
Claudin 3	5′-GAAGCGAGAGATGGGAACTG	5′-GATCTTGGTGGGTGCGTACT	133
Claudin 5	5′-TCTTTGTTACCTTGACCGGC	5′-ACTCCCGGACTACGATGTTG	156
Claudin 7	5′-GGTCTTGCTGCTTTGGTAGC	5′-ACGGTATGCAGCTTTGCTTT	201

Table II. Physicochemical Properties, Permeability Coefficients, and Absorption Properties of the Investigated Drugs in the Training Set[a]

Drug	FA (%)[b]	2/4/A1 $P_c \times 10^6$ (cm/s)	SD	Caco-2 $P_c \times 10^8$ (cm/s)	SD	MW	ClogP	PSA (Å^2)
Acyclovir	16	8.26	±0.82	38.2	±0.45	225	–2.3	119
Atenolol	54	19.5	±2.30	102[c]	±13.2	266	–0.11	92.1
Clodronate	2.5	4.57	±0.40	5.88	±3.63	244	–0.14	138
Creatinine	70	21.5	±1.71	128	±6.76	113	–1.76	92.2
Foscarnet	17	9.56	±0.32	3.50	±1.25	126	–1.78	111
Ganciclovir	5	8.71	±1.47	23.7	±6.66	255	–2.56	132
Lactulose	0.6	8.98	±3.61	27[d]	±6.4	342	–3.59	177
Mannitol	26	11.8	±1.22	12.3	±1.51	182	–2.05	117
Metolazone	64	14.5	±0.54	610[d]	±31	366	2.02	96.0
Raffinose	0.3	5.95	±0.32	5.00	±0.60	504	–8.09	263
Sulpiride	36	11.5	±1.42	39[d]	±5.4	341	1.11	103
Sulfasalazine	12	9.66	±0.86	16[d]	±2.1	398	3.83	147
Vasopressin	0.5	4.95	±0.44	8.10[e]	±0.80	1100	–3.82	ND[f]
PEG 4000	0	5.55	±0.1	4.00	±0.5	4000	ND[f]	ND[f]

[a] Fraction absorbed after oral administration to humans (FA), cellular permeability across 2/4/A1 monolayers ($P_c \pm$ SD), cellular permeability across Caco-2 monolayers ($P_c \pm$ SD), molecular weight (MW), and calculated lipophilicity (ClogP) and polar surface area (PSA) [calculated as described previously (22)] are shown.
[b] Original references obtained from Refs. 22, 44.
[c] Obtained from Ref. 25.
[d] Obtained from Ref. 28.
[e] Obtained from Ref. 45.
[f] ND, not determined.

metformin, nadolol, pravastatin, and lobucavir were obtained from Bristol Myers Squibb (Princeton, NJ).

Permeability of Drugs in 2/4/A1 and Caco-2 Cell Monolayers

2/4/A1 monolayers cultivated at 39°C for 6–8 days or Caco-2 cell monolayers cultivated at 37°C for 21–35 days were used in the drug transport experiments. All transport experiments were performed in Hank's balanced salt solution (HBSS) at pH 7.4 on both the apical and basolateral side at 37°C, as described previously (25). Briefly, for experiments in the apical-to-basolateral direction (a-b), 0.4 ml HBSS containing the drug was added to the apical chamber, for 2/4/A1, at 0.1 mM for the completely absorbed drugs and at 1 mM for the sparingly and intermediately absorbed drugs. The drug concentrations for Caco-2 were 0.1 mM for the completely absorbed drugs and 5 mM for the sparingly and intermediately absorbed drugs. The higher concentrations of drugs used in experiments with Caco-2 as compared to 2/4/A1 cell monolayers were required to obtain detectable concentrations in the receiver chamber. Radiolabeled drugs and markers were used at 1000 to 10,000 Bq/ml with the addition of 0.1 mM unlabeled compound. For experiments in the basolateral-to-apical direction (b-a), 1.2 ml HBSS containing the drug was added to the basolateral chamber at the same concentrations as stated above. Samples were withdrawn from the receiver side at regular time intervals: every 15–30 min for

Table III. Predictability of 2/4/A1 and Caco-2 Cell Monolayers for the Test Set of Intermediately Absorbed Drugs[a]

Drug	FA (%)[b]	2/4/A1 $P_c \times 10^6$ (cm/s)	SD	Predicted FA 2/4/A1 (%)	Caco-2 $P_c \times 10^8$ (cm/s)	SD	Predicted FA Caco-2 (%)	MW	ClogP	PSA (Å^2)
Metformin	56	20.9	±4.13	65	66.4	±16.4	41	129	–1.48	84.39
Lobucavir	50	14.0	±2.11	34	88.7	±13.3	52	265	–2.69	139.87
Didanosine	42	14.6	±0.70	37	25.2	±10.3	13	236	–1.98	99.16
Pravastatin	34	7.73	±0.39	7.3	12.3	±4.65	4.7	424	2.08	119.32
Nadolol	30	14.4	±2.70	36	28.6	±3.79	16	309	0.38	83.44
BMS 187745	NR[c]	13.2	±2.20	30	ND[d]		ND[d]	386	ND[d]	ND[d]
BMS 189664	NR[c]	10.9	±2.10	19	27.4	±5.60	15	479	ND[d]	ND[d]
			$RMSE_{test}$ (%)	15.6		$RMSE_{test}$ (%)	21.1			

[a] Fraction absorbed after oral administration to humans (FA), cellular permeability across 2/4/A1 monolayers ($P_c \pm$ SD), predicted FA in 2/4/A1, cellular permeability across Caco-2 monolayers ($P_c \pm$ SD), predicted FA in Caco-2, molecular weight (MW), and calculated lipophilicity (ClogP) and polar surface area (PSA) [calculated as described previously (22)] are shown.
[b] Original references obtained from Ref. 44 or Chong (unpublished results).
[c] NR, not reported.
[d] ND, not determined. The solubility of BMS 187745 in HBSS was too low to allow for an accurate determination of P_c in Caco-2 cells.

experiments in 2/4/A1 and every 30–45 min for experiments in Caco-2. These samples were replaced with fresh preheated HBSS. Samples containing unlabeled drugs were kept at –20°C pending HPLC analysis, whereas samples containing radiolabeled drugs were analyzed immediately in a liquid scintillation counter.

In order to obtain drug permeability coefficients (P_c) that were unaffected by the unstirred water layer (UWL), the filters were agitated on a calibrated plate shaker (IKA® Shüttler MTS4) at two different stirring rates, 100 rpm and 500 rpm as described previously (26).

The efflux ratio [defined as (b-a/a-b)] was less than 2 for all drugs in both cell models, which shows that active transport was negligible under the experimental conditions (27) (data not shown). The exception was sulfasalazine, which had an efflux ratio of 12 in Caco-2 cell monolayers. However, it has been shown that the efflux of sulfasalazine did not affect the permeability in the a-b direction (28).

Analytic Methods

Radioactive samples were analyzed using a liquid scintillation counter (Packard Instruments 1900CA TRI-CARB®; Canberra Packard Instruments, Downers Grove, IL). Unlabeled samples were analyzed using a binary HPLC system (Bischoff Analysentechnik und -Geräte GmbH, Leonberg, Germany). The mobile phases were MilliQ:acetonitrile:TFA 99:1.0:0.1% (eluent A) and MilliQ:acetonitrile:TFA 1:99: 0.1% (eluent B). The gradient was programmed for each cycle as follows: a linear gradient from A:B 95:5 to A:B 15:85 over 1 min, followed by A:B 15:85 for 0.5 min, and finally A:B 95:5 for 0.75 min. The analytic column was a Reprosil Pur C8-AQ 3 × 53 mm analysis column. The flow rate was 2.0 ml/min, and the absorbance was monitored at the most suitable UV-absorption wavelength for each compound.

Calculations

The apparent permeability coefficient (P_{app}, cm/s) was determined according to the following equation:

$$P_{app} = \frac{K \cdot V_r}{A} \tag{1}$$

where K is the steady-state change in concentration in the receiver chamber (C_t/C_0) with time (s), C_t is the concentration in the receiver compartment at the end of each time interval, C_0 is the concentration in the apical chamber at the start of each time interval (mole/ml), V_r is the volume of the receiver chamber (ml), and A is the surface area of the filter membrane (cm^2).

The sigmoidal equation:

$$FA = \frac{100}{1 - \left(\frac{P_c}{P_{c50}}\right)^{\gamma}} \tag{2}$$

was fitted to the drug transport data. FA is the fraction of a drug absorbed in humans after oral administration, P_{c50} is the P_c at an FA value of 50% and γ is a slope factor. The equation was fitted to the data by minimizing the unweighted sum of squared residuals.

The molecular hydrodynamic radii of the marker molecules were estimated from the cubic root of the molecular weight of each compound multiplied by a constant K, which was given by the ratio between the radius of mannitol (3.6 Å) and the cubic root of the molecular weight of mannitol (MW 182).

$$r = K \cdot \sqrt[3]{MW} \tag{3}$$

This approximation of molecular radii assumes that all molecules have the same hydrodynamic shape in HBSS at pH 7.4.

The average pore radii of the tight junctions in 2/4/A1 and Caco-2 cells were calculated using the pore-restricted diffusion equation, also named the "Renkin function." This equation describes a mathematical model of the diffusion of a solute in a cylinder (16,29):

$$P_p = \frac{\varepsilon}{\delta} \cdot D \cdot F(r/R) \tag{4}$$

where P_p is the paracellular permeability of the solute, ε is the porosity of the cell monolayer, δ is the tortuousity times the path length, D is the diffusion coefficient and $F(r/R)$ is the Renkin equation where r is the radius of the solute and R is the radius of the cylinder:

$$F(r/R) = \left(1 - \left(\frac{r}{R}\right)\right)^2 \cdot \left(1 - 2.104 \cdot \left(\frac{r}{R}\right) + 2.09 \cdot \left(\frac{r}{R}\right)^3 - 0.95 \cdot \left(\frac{r}{R}\right)^5\right) \tag{5}$$

ε/δ and R are constant for any given cell monolayer. It is thus possible to get an estimate of these constants by measuring the permeability for small hydrophilic molecules and fitting the data to Eq. (4).

Statistics

The results are expressed as mean values ± SD of four monolayers. The root mean square error (RMSE), i.e., the standard error of regression, and the coefficient of determination (r^2) were used to measure how well the sigmoidal equation fit the observations.

Rank correlation coefficients, a measure of the association between two separate rankings of n items, were obtained using Spearman's rank coefficient according to:

$$r_s = 1 - \frac{6 \cdot \sum d^2}{(n^3 - n)} \tag{6}$$

where d is the difference of the two ranks associated with each compound and n is the number of compounds. The value r_s is always between –1 and +1. Large r_s values indicate greater association. Small r_s values indicate less association.

RESULTS

Expression of Tight Junction Components

Occludin was expressed in equal amounts in both undifferentiated 2/4/A1 cells (grown at 33°C) and differentiated 2/4/A1 cells (grown at 39°C) (Fig. 1). In contrast, the expression of the claudins depended on the differentiation level of the 2/4/A1 cells. Claudin 1 was more abundantly expressed in differentiated 2/4/A1 cells grown at 39°C, whereas claudin 3 was more abundantly expressed in undifferentiated 2/4/A1 cells grown at 33°C. Claudin 5 and claudin 7 were not ex-

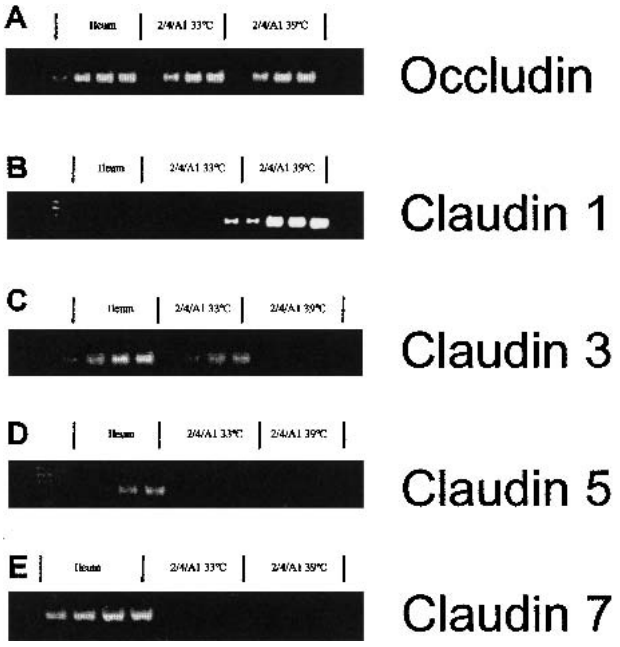

Fig. 1. RT-PCR detection of transcripts of proteins associated with tight junctions in rat ileum and in 2/4/A1 cell monolayers grown at 33°C and 39°C. The RT-PCR reaction was run 25, 29, 33, or 37 cycles for each of the three samples. The cDNA products were loaded on a 2.5% agarose gel, and gene-specific products were detected by ethidium bromide. Occludin (A), claudin 1 (B), claudin 3 (C), claudin 5 (D), and claudin 7 (E) are shown.

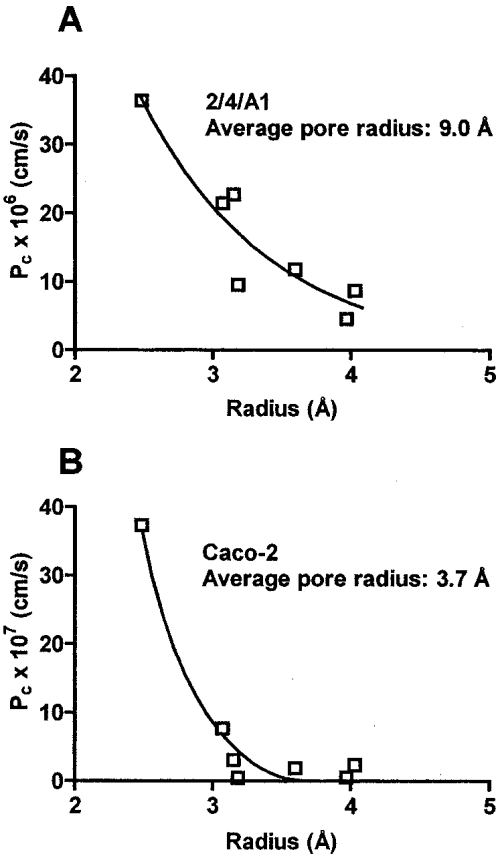

Fig. 2. Determination of average pore radii in 2/4/A1 and Caco-2 cell monolayers. The permeability coefficients of urea (MW 60), creatinine (MW 113), erythritol (MW 122), mannitol (MW 182), foscarnet (MW 126), clodronate (MW 244), and lactulose (MW 342) were determined in 2/4/A1 (A) and Caco-2 (B) cell monolayers. The effective hydrodynamic radii of the molecules were determined using Eq. (3). The two curves represent the best fit to Eq. (4) in the respective cell model ($n = 4$).

pressed in the 2/4/A1 cells, although they were expressed in the rat ileum. Claudins 1 and 3 were also expressed in the rat ileum and in the human intestine (Table IV).

Transport of Hydrophilic Marker Molecules and Calculation of Pore Radii

The permeability to the paracellular marker molecules of 2/4/A1 and Caco-2 monolayers differed both qualitatively and quantitatively (Fig. 2). Although both cell models discriminated the paracellular markers in a size-dependent manner, the P_c values were 10- to 190-fold higher in 2/4/A1 than in Caco-2 cell monolayers, and the fitted curve was more shallow in 2/4/A1 than in Caco-2 cell monolayers (Fig. 2). The difference in paracellular permeability between 2/4/A1 and Caco-2 cell monolayers was quantified by the calculation of the average pore radii in the two cell models using Eq. (4). Average pore radii of 9.0 ± 0.2 Å and 3.7 ± 0.1 Å were obtained for 2/4/A1 and Caco-2 cell monolayers, respectively.

Transport of Passively Absorbed Drugs

We had selected the drugs for this study with the aim of obtaining a wide range of physicochemical properties. We

Table IV. Relative Expression of mRNA of Genes Associated with the Tight Junctions in Rat Ileum, 2/4/A1 at 33°C and 39°C, and in the Human Intestinal Epithelium

Tight junction protein	Expression in rat ileum	Expression in 2/4/A1 33°C	Expression in 2/4/A1 39°C	Expression in the human intestinal epithelium[a]
Occludin	+++	+++	+++	Y
Claudin 1	+	++	+++	Y
Claudin 2	ND[c]	ND[c]	ND[c]	Y
Claudin 3	+++	++	+	Y
Claudin 5	+++	–	–	N
Claudin 7	+++	–	–	NR[b]

[a] Reported from literature: Y, expressed; N, not expressed; occludin (42), claudin 1 (43), claudin 2, 3, and 5 (29,32).
[b] NR, not reported.
[c] ND, not determined.

confirmed that this was the case by carrying out principal component analysis of the drug properties. The even distribution of the drugs in the physicochemical space (Fig. 3) shows that the drugs were indeed structurally diverse.

The general performance of 2/4/A1 monolayers was studied using 20 structurally diverse drug molecules that have an absorbed fraction after oral administration to humans (FA) ranging from 0 to 100%. Although we previously have performed similar studies (9), the introduction of the new cell culture procedure motivated this experiment. The results are presented in Fig. 4 and show that sigmoidal relationships were obtained for both 2/4/A1 and Caco-2 cell monolayers. However, when the drugs were categorized as sparingly (FA 0–20%), intermediately (FA 20–80%), and completely (80–100%) absorbed drugs (23), the P_c values for sparingly and intermediately absorbed drugs (hereafter denoted incompletely absorbed drugs) appeared more scattered in Caco-2 than in 2/4/A1 cell monolayers.

Transport of Incompletely Absorbed Drugs

Results from the 13 incompletely absorbed drugs (FA 0–80%) in Fig. 4 were extracted and used to establish relationships between FA and P_c for the 2/4/A1 and Caco-2 monolayers. As can be seen in Table II, the P_c values of the 13 drugs ranged from 4.57×10^{-6} cm/s for clodronate (FA = 2.5%) to 21.5×10^{-6} cm/s for creatinine (FA = 70%), or a factor of 5. A strong sigmoidal relationship between P_c and FA was obtained for the training set in 2/4/A1 ($R^2_{training}$ = 0.95, $RMSE_{training}$ = 5.37%) (Fig. 5A). The P_c values for Caco-2 monolayers ranged from 3.5×10^{-8} cm/s for foscarnet (FA = 17%) to 610×10^{-8} cm/s for metolazone (FA = 64%), or a factor of 174. Despite that the P_c values covered a larger range in the Caco-2 monolayers, a weaker relationship between FA and P_c was obtained ($R^2_{training}$ = 0.82, $RMSE_{training}$ = 10.14%) (Fig. 5B).

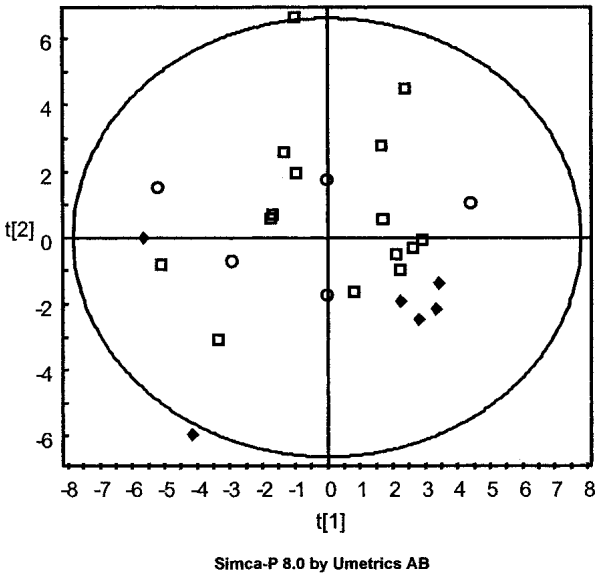

Fig. 3. Score scatter plot showing t1 against t2 for the training set *(squares),* test set *(circles),* and completely absorbed drugs *(filled diamonds)*. The principal components were constructed from the calculated descriptors: molecular weight, surface area, volume, ClogP, $NPSA_{saturated}$, $NPSA_{unsaturated}$, NPSA, PSA, and fraction PSA.

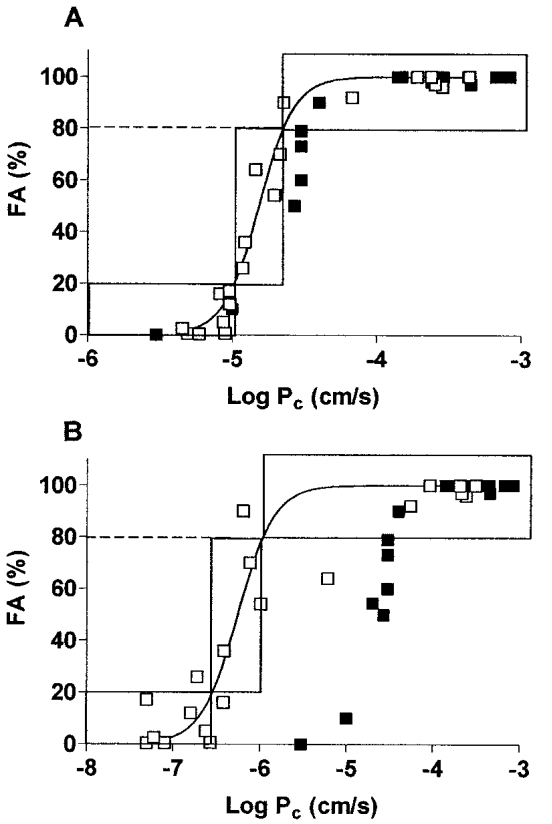

Fig. 4. Relationships between FA and permeability coefficients *(open symbols)* obtained in 2/4/A1 (A) and Caco-2 (B). *Closed symbols* represent data from the human jejunum *in vivo* (41). The *squares* represent sparingly absorbed (FA 0–20%), intermediately absorbed (FA 20–80%) and completely absorbed (80–100%) drugs after oral administration to humans. The two curves represent the best fit to Eq. (2).

The sigmoidal relationships for the 13 drugs in Fig. 5 were used to predict the FAs of a further seven incompletely absorbed drugs (defined as an *ad hoc* test set) (Table III). The selection of these compounds was based on the observation that their FA values are particularly difficult to predict using Caco-2 cell monolayers (Saeho Chong, unpublished results). Note that these drugs were equally well distributed with regard to molecular properties as were the 13 drugs in the training set (Fig. 3). The P_c values of the drugs in the *ad hoc* test set (Table III) ranged from 7.73×10^{-6} cm/s for pravastatin (FA = 34%) to 20.9×10^{-6} cm/s for metformin (FA = 56%) in 2/4/A1, or a factor of 2.7 (Fig. 5A). In Caco-2 cells the P_c values ranged from 12.3×10^{-8} cm/s for pravastatin to 88.7×10^{-8} cm/s for lobucavir (FA = 50%), or a factor of 7.2 (Fig. 5B). BMS 187745 (31) and BMS 189664 were excluded from the data set because no FA values were available from Bristol Myers Squibb. However, the predicted FA values for BMS 187745 and BMS 189664 using 2/4/A1 monolayers were 30% and 19%, respectively (Table III). The P_c of BMS 187745 could not be reliably determined in Caco-2 because the compound was transported in insufficient amounts to be detected by the HPLC method used in this study. BMS 194664 is more soluble than BMS 187745, and its predicted FA in Caco-2 cell monolayers is 15%. The average errors in the prediction of FA for the remaining five drugs in the test set were $RMSE_{test}$ = 15.6 and 21.1 for 2/4/A1 and Caco-2, respectively, which

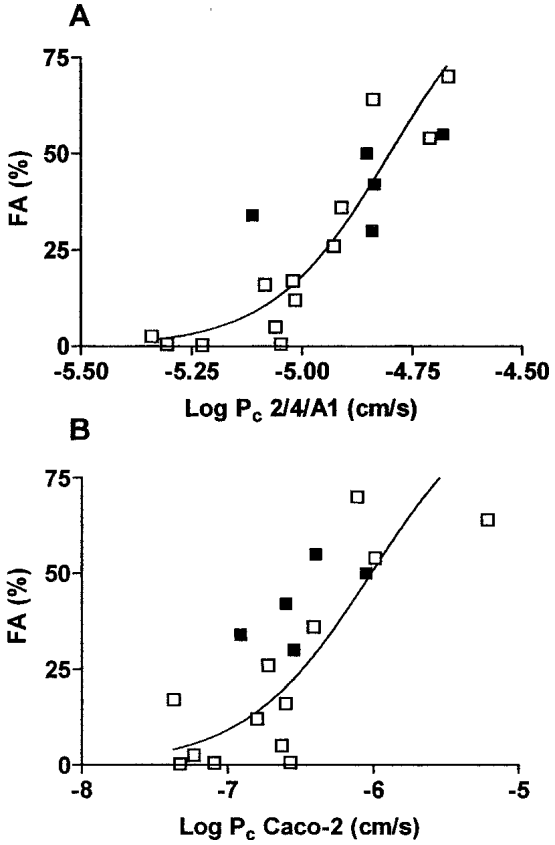

Fig. 5. Sigmoidal relationships between FA and permeability coefficients in 2/4/A1 (A) and Caco-2 (B) cell monolayers. *Open symbols* represent drugs in the training set (Table II), and *solid symbols* represent drugs in the *ad hoc* test set (Table III). The two curves represent the best fit to Eq. (2) for the training set.

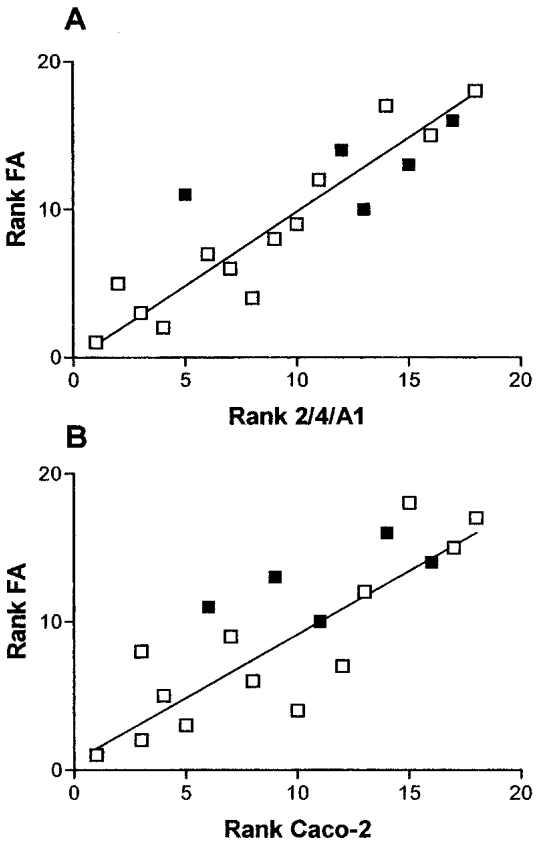

Fig. 6. Spearman's rank coefficient of FA vs. P_c in 2/4/A1 (A) and in Caco-2 (B) for the incompletely absorbed drugs (FA 0–80%). Lower rank corresponds to lower FA and P_c. *Open symbols* represent the 13 drugs in the training set, and *closed symbols* represent the drugs (with known FA) in the *ad hoc* test set.

shows that 2/4/A1 cell monolayers predict the FAs of incompletely absorbed drugs better than Caco-2 cell monolayers.

Analysis of the ranking of the predicted FA values from the P_c values in the two cell culture models (Fig. 6) supports this conclusion. Spearman's rank coefficient was significantly higher ($p < 0.05$) for FA vs. P_c in 2/4/A1 (0.90) than it was for FA vs. P_c in Caco-2 (0.75) for the incompletely absorbed drugs.

DISCUSSION

2/4/A1 cells expressed occludin and claudins at the transcriptional level. However, the expression pattern of the claudins was qualitatively different from the expression pattern in the rat ileum. Although 2/4/A1 cells, rat ileum, and human intestine all expressed occludin, claudin 1, and claudin 3, only rat ileum expressed claudins 5 and 7 at appreciable levels. It must be remembered that the intestinal tissue contains not only epithelial cells but also other cell types, including blood vessel endothelial cells. The expression of claudin 5 in the intestinal tissues most likely originated from the blood vessel endothelium rather than the intestinal epithelium (30). We could not find any explanation for the variable expression of claudin 7, but note that the cellular distribution of this claudin is not yet known. Clearly, additional studies of the expression and function of claudin 7 are required before any firm conclusions can be drawn regarding the importance of the expression of this claudin in epithelia. Interestingly, the expression patterns of claudins in 2/4/A1 cells changed with culture temperature. We speculate that this shift, which included the down-regulation of claudin 3 and up-regulation of claudin 1, corresponds to the higher transepithelial electrical resistance (TER) ($50 \pm 6\ \Omega \times cm^2$) of 2/4/A1 cell monolayers grown at 39°C (8) than of 2/4/A1 cell monolayers grown at 33°C (TER = $15 \pm 2\ \Omega \times cm^2$).

Another interesting claudin is claudin 2, which was expressed in the low-resistance cell line Madin–Darby canine kidney (MDCK) II but was not expressed in the high-resistance MDCK I (32). Furthermore, it was shown that transfection of MDCK I monolayers with claudin 2 changed these monolayers from high to low resistance. Claudin 2 is predominantly expressed in epithelial cells lining the wall of the villus (33) [which are known to form larger aqueous pores than those formed between the epithial cells at the tip of the villus (34)] but not in differentiated enterocytes at the villus tip. Thus, differential expression of claudin 2 has been associated with changes in resistance of the tight junctions, and it would therefore have been interesting to study the temperature-dependent expression of claudin 2 in 2/4/A1. These studies will be undertaken as soon as the sequence of rat claudin 2 becomes available. We can conclude on the basis of the results presented here that 2/4/A1 cells express some of the epithelial-specific claudins found in the rat and human small intestine.

At the functional level, the average pore radius of 2/4/A1

cell monolayers (9.0 Å) was in close agreement with that reported in the human small intestine (8–13 Å) (35). In a more recent study (34), it was shown that the average pore radius of the most apical part of the villus of the rat small intestine contains small pores (radius <6 Å), whereas the basal part of the villus contains larger pores (10–15 Å). Results from perfusion studies using the Loc-I-Gut technique also support the existence of a dual pore system for the absorption of hydrophilic molecules in the human jejunum (36). Together, these results provide evidence for the existence of a second paracellular route that is sufficiently large to allow the passage of drug-like molecules in the rat and human small intestines. Because Caco-2 cell monolayers have an average pore radius of less than 6 Å, we speculate that the paracellular route of these cell monolayers represents the most apical part of the villus epithelium (37), whereas 2/4/A1 cell monolayers are more representative of the lower parts of the villus. It remains to be shown if cocultures of 2/4/A1 and Caco-2 form tight monolayers with the two distinct pore-size distributions found *in vivo*.

We note that the striking quantitative overlap between drug permeability in 2/4/A1 and that found in the human small intestine *in vivo* (Fig. 4) may not solely be explained by the *in vivo*-like pore radii of these cells. It is well known that the absorptive surface areas differ between cell cultures and intestinal tissues because cell cultures grow as flat cell layers and the intestinal epithelium grows on folded structures, so the effective absorptive area may be larger *in vivo* than that in the cell cultures (38). However, the surface-enlarging intestinal folds are generally not taken into account in studies of drug permeability in the intestine *in vivo* (39,40).

The difference between the P_c values for incompletely and completely absorbed drugs was much smaller in 2/4/A1 than in Caco-2 cell monolayers. This fact may be explained by the larger contribution of the paracellular pathway to the overall permeability in 2/4/A1 monolayers. This resulted in a less scattered relationship between FA and P_c for 2/4/A1 than for Caco-2 for the low-permeability drugs and in better predictions of FA in 2/4/A1 than in Caco-2. However, this finding must be confirmed with larger data sets. Most importantly, the range in P_c values obtained in 2/4/A1 cell monolayers is in excellent agreement with that obtained in the human jejunum (41). This suggests that the more leaky pores recently found in the rat and human small intestines (34,35) are more significant for intestinal drug absorption than previously recognized.

We conclude that 2/4/A1 cell monolayers have a small intestine-like permeability and that these cell monolayers predicted the intestinal absorption of a set of low-permeability drugs that are incompletely absorbed better than did Caco-2 cell monolayers. Additional advantages of the 2/4/A1 model as compared to Caco-2 include a shorter cultivation time (4–6 days compared to 21 days for Caco-2 cells using the standard cell culture procedure) and (because larger amounts of drugs are transported in 2/4/A1 cells) improved precision in the analysis of transported drug, as exemplified by the studies of BMS 187745.

ACKNOWLEDGMENTS

This work was supported by the Swedish Research Council (9478), The Swedish National Board for Laboratory Animals (97-46), and Bristol-Myers Squibb.

REFERENCES

1. P. Artursson and R. T. Borchardt. Intestinal drug absorption and metabolism in cell cultures: Caco-2 and beyond. *Pharm. Res.* **14**: 1655–1658 (1997).
2. A. K. Mandagere, T. N. Thompson, and K. K. Hwang. Graphical model for estimating oral bioavailability of drugs in humans and other species from their Caco-2 permeability and *in vitro* liver enzyme metabolic stability rates. *J. Med. Chem.* **45**:304–311 (2002).
3. W. Rubas, M. E. Cromwell, Z. Shahrokh, J. Villagran, T. N. Nguyen, M. Wellton, T. H. Nguyen, and R. J. Mrsny. Flux measurements across Caco-2 monolayers may predict transport in human large intestinal tissue. *J. Pharm. Sci.* **85**:165–169 (1996).
4. M. C. Gres, B. Julian, M. Bourrie, V. Meunier, C. Roques, M. Berger, X. Boulenc, Y. Berger, and G. Fabre. Correlation between oral drug absorption in humans, and apparent drug permeability in TC-7 cells, a human epithelial intestinal cell line: comparison with the parental Caco-2 cell line. *Pharm. Res.* **15**: 726–733 (1998).
5. G. M. Pauletti, F. W. Okumu, and R. T. Borchardt. Effect of size and charge on the passive diffusion of peptides across Caco-2 cell monolayers via the paracellular pathway. *Pharm. Res.* **14**:164–168 (1997).
6. P. Artursson, A.-L. Ungell, and J.-E. Löfroth. Selective paracellular permeability in two models of intestinal absorption: Cultured monolayers of human intestinal epithelial cells and rat intestinal segments. *Pharm. Res.* **8**:1123–1129 (1993).
7. H. Lennernäs, K. Palm, U. Fagerholm, and P. Artursson. Comparison between active and passive drug transport in human intestinal epithelial (Caco-2) cells *in vitro* and human jejunum *in vivo*. *Int. J. Pharm.* **127**:103–107 (1996).
8. S. Tavelin, J. Taipalensuu, F. Hallböök, K. Vellonen, V. Moore, and P. Artursson. An improved cell culture model based on 2/4/A1 cell monolayers for studies of intestinal drug transport. Characterization of Transport Routes. *Pharm Res*. **20**:373–387 (2003).
9. S. Tavelin, V. Milovic, G. Ocklind, S. Olsson, and P. Artursson. A conditionally immortalized epithelial cell line for studies of intestinal drug transport. *J. Pharmacol. Exp. Ther.* **290**:1212–1221 (1999).
10. A. Collett, E. Sims, D. Walker, Y. L. He, J. Ayrton, M. Rowland, and G. Warhurst. Comparison of HT29-18-C1 and Caco-2 cell lines as models for studying intestinal paracellular drug absorption. *Pharm. Res.* **13**:216–221 (1996).
11. A. Adson, T. J. Raub, P. S. Burton, C. L. Barsuhn, A. R. Hilgers, K. L. Audus, and N. F. Ho. Quantitative approaches to delineate paracellular diffusion in cultured epithelial cell monolayers. *J. Pharm. Sci.* **83**:1529–1536 (1994).
12. L. S. Gan, S. Yanni, and D. R. Thakker. Modulation of the tight junctions of the Caco-2 cell monolayers by H2- antagonists. *Pharm. Res.* **15**:53–57 (1998).
13. K. Lee and D. R. Thakker. Saturable transport of H2-antagonists ranitidine and famotidine across Caco-2 cell monolayers. *J. Pharm. Sci.* **88**:680–687 (1999).
14. V. Pade and S. Stavchansky. Estimation of the relative contribution of the transcellular and paracellular pathway to the transport of passively absorbed drugs in the Caco-2 cell culture model. *Pharm. Res.* **14**:1210–1215 (1997).
15. S. D. Flanagan, L. H. Takahashi, X. Liu, and L. Z. Benet. Contributions of saturable active secretion, passive transcellular, and paracellular diffusion to the overall transport of furosemide across adenocarcinoma (Caco-2) cells. *J. Pharm. Sci.* **91**:1169–1177 (2002).
16. G. T. Knipp, N. F. Ho, C. L. Barsuhn, and R. T. Borchardt. Paracellular diffusion in Caco-2 cell monolayers: effect of perturbation on the transport of hydrophilic compounds that vary in charge and size. *J. Pharm. Sci.* **86**:1105–1110 (1997).
17. Y. L. He, S. Murby, G. Warhurst, L. Gifford, D. Walker, J. Ayrton, R. Eastmond, and M. Rowland. Species differences in size discrimination in the paracellular pathway reflected by oral bioavailability of poly(ethylene glycol) and D-peptides. *J. Pharm. Sci.* **87**:626–633 (1998).
18. E. C. A. Paul, J. Hochman, and A. Quaroni. Conditionally immortalized intestinal epithelial cells. novel approach for study of

differentiated enterocytes. *Am. J. Physiol.* **265**:C266–C278 (1993).
19. P. Artursson. Epithelial transport of drugs in cell culture. I: A model for studying the passive diffusion of drugs over intestinal absorptive (Caco-2) cells. *J. Pharm. Sci.* **79**:476–482 (1990).
20. P. Artursson, J. Karlsson, G. Ocklind, and N. Schipper. Studying transport processes in absorptive epithelia. in *Epithelial Cell Culture-A Practical Approach*, A.J. Shaw, (ed.), Oxford Press, New York, 1996, pp. 111–133.
21. J. Taipalensuu, H. Törnblom, G. Lindberg, C. Einarsson, F. Sjöqvist, H. Melhus, P. Garberg, B. Sjöström, B. Lundgren, and P. Artursson. Correlation of gene expression of ten drug efflux proteins of the atp-binding cassette transporter family in normal human jejunum and in human intestinal epithelial caco-2 cell monolayers. *J. Pharmacol. Exp. Ther.* **299**:164–170 (2001).
22. K. Palm, P. Stenberg, K. Luthman, and P. Artursson. Polar molecular surface properties predict the intestinal absorption of drugs in humans. *Pharm. Res.* **14**:568–571 (1997).
23. S. Winiwarter, N. M. Bonham, F. Ax, A. Hallberg, H. Lennernäs, and A. Karlen. Correlation of human jejunal permeability (*in vivo*) of drugs with experimentally and theoretically derived parameters. A multivariate data analysis approach. *J. Med. Chem.* **41**:4939–4949 (1998).
24. C. A. Bergström, U. Norinder, K. Luthman, and P. Artursson. Experimental and computational screening models for prediction of aqueous drug solubility. *Pharm. Res.* **19**:182–188 (2002).
25. K. Palm, K. Luthman, A. L. Ungell, G. Strandlund, F. Beigi, P. Lundahl, and P. Artursson. Evaluation of dynamic polar molecular surface area as predictor of drug absorption: comparison with other computational and experimental predictors. *J. Med. Chem.* **41**:5382–5392 (1998).
26. J. Karlsson and P. Artursson. A new diffusion chamber system for the determination of drug permeability coefficients across the human intestinal epithelium that are independent of the unstirred water layer. *Biochim. Biophys. Acta* **1111**:204–210 (1992).
27. J. W. Polli, S. A. Wring, J. E. Humphreys, L. Huang, J. B. Morgan, L. O. Webster, and C. S. Serabjit-Singh. Rational use of *in vitro* P-glycoprotein assays in drug discovery. *J. Pharmacol. Exp. Ther.* **299**:620–628 (2001).
28. P. Stenberg, U. Norinder, K. Luthman, and P. Artursson. Experimental and computational screening models for the prediction of intestinal drug absorption. *J. Med. Chem.* **44**:1927–1937 (2001).
29. F. Curry. Mechanics and Thermodynamics of Transcapillary Exchange, in *Handbook of Physiology*, E. Renkin and C. Michel (eds.), American Physiological Society, Bethesda, 1984, pp. 309–374.
30. K. Morita, H. Sasaki, M. Furuse, and S. Tsukita. Endothelial claudin: claudin-5/TMVCF constitutes tight junction strands in endothelial cells. *J. Cell Biol.* **147**:185–194 (1999).
31. A. Sharma, P. H. Slugg, J. L. Hammett, and W. J. Jusko. Estimation of oral bioavailability of a long half-life drug in healthy subjects. *Pharm. Res.* **15**:1782–1786 (1998).
32. M. Furuse, K. Furuse, H. Sasaki, and S. Tsukita. Conversion of zonulae occludentes from tight to leaky strand type by introducing claudin-2 into Madin-Darby canine kidney I cells. *J. Cell Biol.* **153**:263–272 (2001).
33. C. Rahner, L. L. Mitic, and J. M. Anderson. Heterogeneity in expression and subcellular localization of claudins 2, 3, 4, and 5 in the rat liver, pancreas, and gut. *Gastroenterology* **120**:411–422 (2001).
34. B. M. Fihn, A. Sjöqvist, and M. Jodal. Permeability of the rat small intestinal epithelium along the villus- crypt axis: effects of glucose transport. *Gastroenterology* **119**:1029–1036 (2000).
35. K. D. Fine, C. A. Santa Ana, J. L. Porter, and J. S. Fordtran. Effect of changing intestinal flow rate on a measurement of intestinal permeability. *Gastroenterology* **108**:983–989 (1995).
36. J. D. Söderholm, G. Olaison, A. Kald, C. Tagesson, and R. Sjödahl. Absorption profiles for polyethylene glycols after regional jejunal perfusion and oral load in healthy humans. *Dig. Dis. Sci.* **42**:853–857 (1997).
37. S. Yamashita, Y. Tanaka, Y. Endoh, Y. Taki, T. Sakane, T. Nadai, and H. Sezaki. Analysis of drug permeation across Caco-2 monolayer: implication for predicting in vivo drug absorption. *Pharm. Res.* **14**:486–491 (1997).
38. P. Artursson, K. Palm, and K. Luthman. Caco-2 monolayers in experimental and theoretical predictions of drug transport. *Adv. Drug Deliv. Rev.* **46**:27–43 (2001).
39. L. Knutson, B. Odlind, and R. Hällgren. A new technique for segmental jejunal perfusion in man. *Am. J. Gastroenterol.* **84**: 1278–1284 (1989).
40. D. Nilsson, U. Fagerholm, and H. Lennernäs. The influence of net water absorption on the permeability of antipyrine and levodopa in the human jejunum. *Pharm. Res.* **11**:1540–1547 (1994).
41. H. Lennernäs. Human jejunal effective permeability and its correlation with preclinical drug absorption models. *J. Pharm. Pharmacol.* **49**:627–638 (1997).
42. M. Furuse, T. Hirase, M. Itoh, A. Nagafuchi, S. Yonemura, and S. Tsukita. Occludin: a novel integral membrane protein localizing at tight junctions. *J. Cell Biol.* **123**:1777–1788 (1993).
43. T. Kucharzik, S. V. Walsh, J. Chen, C. A. Parkos, and A. Nusrat. Neutrophil transmigration in inflammatory bowel disease is associated with differential expression of epithelial intercellular junction proteins. *Am. J. Pathol.* **159**:2001–2009 (2001).
44. Y. H. Zhao, J. Le, M. H. Abraham, A. Hersey, P. J. Eddershaw, C. N. Luscombe, D. Butina, G. Beck, B. Sherborne, I. Cooper, J. A. Platts, and D. Boutina. Evaluation of human intestinal absorption data and subsequent derivation of a quantitative structure-activity relationship (QSAR) with the Abraham descriptors. *J. Pharm. Sci.* **90**:749–784 (2001).
45. T. Lindmark, N. Schipper, L. Lazorova, A. G. de Boer, and P. Artursson. Absorption enhancement in intestinal epithelial Caco-2 monolayers by sodium caprate: assessment of molecular weight dependence and demonstration of transport routes. *J. Drug Target.* **5**:215–223 (1998).